Supercritical loading of gatifloxacin into hydrophobic foldable intraocular lenses - Process control and optimization by following in situ CO2 sorption and polymer swelling

Kanjana Ongkasin, Yasmine Masmoudi, Thierry Tassaing, Gwenaelle Le-Bourdon, Elisabeth Badens

Supercritical loading of gatifloxacin into hydrophobic foldable intraocular lenses – Process control and optimization by following *in situ* CO_2 sorption and polymer swelling

Kanjana Ongkasin[a,b], Yasmine Masmoudi[a,b,*], Thierry Tassaing[b,c], Gwenaelle Le-Bourdon[b,c], Elisabeth Badens[a,b]

[a] *Aix Marseille Univ, CNRS, Centrale Marseille, M2P2 Marseille, France*
[b] *Franco-Chinese Research Center on Supercritical Fluid Technology Applied to Vision Science, France*
[c] *Université de Bordeaux, ISM, UMR CNRS 5255, Talence 33405, France*

ARTICLE INFO

Keywords:
Supercritical carbon dioxide (CO_2)
impregnation
Therapeutic intraocular lenses
Endophthalmitis mitigation
Gatifloxacin
In-situ FTIR analyzis
CO_2 sorption
Polymer swelling

ABSTRACT

The supercritical impregnation process was used as a green technology for the elaboration of drug delivery intraocular lenses to mitigate the risk of post-operatory endophthalmitis after cataract surgery. Commercially available hydrophobic acrylic (copolymer of benzyl methacrylate and methyl methacrylate) intraocular lenses (IOLs) were impregnated with gatifloxacin, a fourth generation fluoroquinolone drug, using pure supercritical CO_2 ($scCO_2$) to obtain solvent-free loaded implants. The interaction phenomena involved in the supercritical impregnation were studied by following *in situ* $scCO_2$ sorption within the polymer support and the subsequent IOL swelling, and by taking into account drug solubility in the supercritical fluid phase. The drug impregnation yields determined though *in-vitro* release studies varied between 0.33 and 1.07 ± 0.07 $\mu g \cdot mg_{IOL}^{-1}$ in the studied experimental conditions (8 to 25 MPa, 308 to 328 K and 30 to 240 min impregnation duration). An impregnation duration longer or equal to the time required for a complete CO_2 uptake by the polymer as well as a higher pressure or a higher temperature over the crossover pressure delimiting the upper limit of the retrograde solubility zone, led to higher drug impregnation yields.

1. Introduction

Cataract is the most common cause of blindness and the second cause of moderate and severe vision impairment worldwide (Varadaraj et al., 2019). According to a recent systematic review and meta-analysis conducted on behalf of the Vision Loss Expert Group of the Global Burden of Disease Study, cataract was responsible for 24% of moderate and severe vision impairments (52.6 million out of 216.6 million patients) and 35% of blindiness (12.6 million out of 36.0 million) in 2015 (Flaxman et al., 2017). Cataract blindness can be avoided only through surgical intervention which restores visual impairment by replacing the opacified natural crystalline lens with an artificial one, commonly made from hydrophobic or hydrophilic polymers and less commonly from silicone (Findl, 2009). Thanks to recent developments in material sciences and surgical procedures, only small incision surgery is required to insert the foldable intraocular lense, thus improving recovery time and significantly reducing the incidence of postoperative complications (Kohnen and Koch, 2005; Rengaraj et al., 2016). Even if cataract surgery is generally considered as safe, severe postoperative complications may occur. One of the most devastating is endophthalmitis, an intraocular inflammatory disorder affecting the vitreous cavity resulting from spread of infecting organisms into the eye (Kernt and Kampik, 2010), although these cases are rare with incidences varying from 0.03 to 0.2% across the world (Kohnen and Koch, 2005; Javitt, 2016; Garg et al., 2017).

In order to prevent short and long-term complications from endophthalmitis, the injection of anti-inflammatory or antibiotic drugs (subconjunctival, topical, intracameral or intravitreal) is carried out at the end of surgery (Das and Sharma, 2018). Fluoroquinolone antibiotics are the most commonly used antimicrobials for the prevention and management of bacterial endophthalmitis (Miller, 2006; Alhusban et al., 2019).

Arantes et al. (2008) have applied fluoroquinolone eye drops of either gatifloxacin (a fourth generation fluoroquinolone), or ciprofloxacin (a second generation fluoroquinolone) one hour before and 14 days after cataract surgery. The efficacy of gatifloxacin in reducing

* Corresponding author at: Aix Marseille Univ, CNRS, Centrale Marseille, M2P2 Marseille, France.
E-mail address: yasmine.masmoudi@univ-amu.fr (Y. Masmoudi).

the number of positive post-operative conjunctival cultures has been shown to be superior to that of ciprofloxacin, indicating its efficacy in reducing post-operative infections. The efficiency of gatifloxacin, was also found to be superior to that of ceftriaxone, cefepime and vancomycin in treating a strain of penicillin-resistant *Streptococcus pneumoniae in-vitro*, in a rabbit model (Perrig et al., 2001). Futhermore, based on the rabbit model results, gatifloxacin was shown to present a better bactericidal activity than trovafloxacin (Rodoni et al., 1999) and grepafloxine (Gerber, 2000), both also being fourth generation fluoroquinolones. Although gatifloxacin was banned for use in oral dosage form because of toxicity issues, no systemic toxicity was observed in topical ophthalmic applications (Jensen et al., 2008; Schultz, 2012) and it is still recommended for the prophylaxis of postoperative endophthalmitis (Jensen et al., 2008). According to the 2014 survey by the American Society of Cataract and Refractive Surgery, 90% of respondent surgeons apply topical perioperative antibiotic prophylaxis at the time of surgery, with 60% preferring gatifloxacin or moxifloxacin fourth generation fluoroquinolone (Chang et al., 2015).

The elaboration of sustained-release drug delivery systems is an effective way to improve drug formulation and administration protocols while enhancing the therapeutic efficiency, achieving cell targeting and avoiding overdose risks. The practice of loading drugs into modern ocular supports has expanded in the last decades in the treatment of various eye diseases such as as glaucoma, posterior capsule opacification (PCO) or endophtalmitis. Several methodologies have been applied such as soaking in liquids (Matsushima et al., 2005; Li and Chauhan, 2006; Kugelberg et al., 2010; Eibl et al., 2013; Wertheimer C et al., 2015; Phan et al., 2016; Topete et al., 2018), molecular imprinting (Hiratani et al., 2005; Maulvi et al., 2019), surface modification (Wang et al., 2015), electrospinning (Mehta et al., 2017), incorporating drugs into colloidal structures, dispersing nanoparticles or microparticles in the polymeric network of lenses (Gulsen and Chauhan, 2004, 2005; Kapoor et al., 2009; Jung et al., 2013), grafting or inbuilding (co-polymerization) cyclodextrins into lenses to host drugs by forming dynamic inclusion complexes (Rodriguez-Tenreiro et al., 2006; Ribeiro et al., 2012), formulating liposomes (Danion et al., 2007a, 2007b, 2007c; Jain and Shastri, 2011) or loading contact lenses with microemulsions (Li et al., 2007), etc.

The aforementioned listed methodologies generally imply the use of often toxic organic solvents. In spite of the application of several separation procedures for their elimination, residual traces can still remain inside the final products and can be problematic for the sensitive tissues in the eye. Furthermore, drug/solvent dissolution and compatibility as well as drug degradation (thermal, photochemical, etc.) issues can also occur. In the conventional impregnation process (soaking method), low diffusion rates imply long impregnation duration and limited diffusion depth (Weidner, 2018).

An alternative for the elaboration of sustained-release drug delivery systems is the use of the supercritical impregnation process. For several years, supercritical fluid technologies have been attracting a growing interest in the pharmaceutical and biomedical fields (Davies et al., 2008; Duarte et al., 2009; Badens et al., 2018; Matos et al., 2019). As underlined by several studies, supercritical CO_2 ($scCO_2$) is an attractive impregnation carrier, thanks notably to its enhanced transfer phenomena compared to that of liquid solvents (lower viscosity, higher diffusivity and surface tension close to zero). Transfer phenomena are further promoted by $scCO_2$ sorption within polymers favoring their reversible swelling and resulting in shorter processing durations with homogeneous and in-depth impregnation (Bouledjouidja et al., 2017a; Barros et al., 2017; Champeau et al., 2015b; Kikic and Vecchione, 2003; Kazarian, 2000). A key parameter governing supercritical impregnation is the partitioning of the solute between the fluid phase and the impregnation support. A molecular dispersion of the drug within the polymeric support can be obtained, even if its solubility in $scCO_2$ is low (Kazarian, 2004; Kazarian et al., 1998; Pasquali and Bettini, 2008). As $scCO_2$ is spontaneously released at the end of the process upon depressurization, solvent free end-products meeting regulatory requirements for pharmaceutical and biomedical applications can be obtained. For these fields, the mild critical temperature of CO_2 (31 °C) allowing the processing of thermosenstive compounds as well as its biocidal properties are also of interest (Soares et al., 2019).

The process is considered adjustable since the impregnation yield as well as the drug release can be controlled by varying the operating conditions to obtain sustained drug release varying from a few hours to several weeks. Indeed, several concomitant interaction phenomena are involved in the impregnation process; the sorption of $scCO_2$ in the polymer support and the resulting swelling of the latter, the solubilization of the drug in supercritical CO_2 and its partitioning between the polymer and the fluid phase according to relative affinities. All these interactions can be influenced by varying the operating conditions of pressure, temperature and impregnation duration. Their influence on impregnation are therefore complex to predict, and contradictory results have been reported in the literature depending on the polymer and drug components involved (Bouledjouidja et al., 2016; Bouledjouidja et al., 2017b; Champeau et al., 2015b; Fleming and Kazarian, 2005; Kazarian, 2004; Kikic and Vecchione, 2003; Pasquali and Bettini, 2008; Üzer et al., 2006).

The supercritical fluid impregnation process has been successfully applied to the elaboration of ophthalmic localized sustained-release drug delivery intraocular lenses or contact lenses (Braga et al., 2011; Costa et al., 2010; Dias et al., 2011; Duarte et al., 2007, 2008; Bouledjouidja et al., 2016, 2017b; Masmoudi et al., 2011; Yokozaki et al., 2015a, 2015b; Yokozaki and Shimoyama, 2018). Some of these studies feature the feasability of obtaining effective and in-depth impregnation within these sensitive medical devices without altering their thermomechanical, surface/wettability, oxygen permeability and optical properties (Masmoudi et al., 2011; Braga et al., 2011; Bouledjouidja et al., 2017a, 2017b; Costa et al., 2010).

The present work is a part of a larger research project for the elaboration of sustained-release drug delivery intraocular lenses through supercritical impregnation to prevent postoperative complications of cataract surgery. More precisely, in this study, gatifloxacin, a bactericidal antibiotic of the fourth-generation fluoroquinolone family was loaded into commercially available hydrophobic foldable IOLs for the prevention of endophthalmitis. The originality of this work is to investigate the different mechanisms involved in supercritical impregnation to better explore the influence of operating conditions and to improve the understanding and the optimization of the process. For that purpose, CO_2 sorption within polymer IOLs and the subsequent swelling of the latter were determined by carrying out *in situ* Fourier transform infrared micro-spectroscopy (FTIR) measurements. By following the kinetic of CO_2 sorption online, it was also possible to determine the time required to reach thermodynamic equilibrium, which is an important data to understand the influence of impregnation duration. In addition to this, the drug solubility in supercritical CO_2 was calculated (using results from the literature) and its partition coefficent between the polymer and the fluid phase determined in the different experimental conditions of pressure and temperature. The variation of the drug impregnation yield has been discussed refering to all these data.

2. Material and methods

2.1. Chemicals

Commercially available foldable hydrophobic acrylic (copolymer of benzyl methacrylate and methyl methacrylate) IOLs were kindly provided by Shenyang Bio Medical Device Co. Ltd. and He Eye Care System (Liaoning Province, China). They present diopters varying between 21 and 22 + D.

Carbon dioxide (99.7% purity) was supplied by Air Liquide (France). Gatifloxacin ($C_{19}H_{22}FN_3O_4$, 375.39 $g.mol^{-1}$) was purchased from Sigma-Aldrich (France) and was stored at −20 °C. Its skeletal

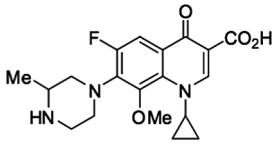

Fig. 1. Skeletal formula of gatifloxacin.

formula is illustrated in Fig. 1.

2.2. Solubility of gatifloxacin in supercritical CO_2

Gatifloxacin solubility in supercritical CO_2 (y_{GTX}) was studied by Shi et al. (2017) Experimental measurements were carried out at three temperatures 313, 323 and 333 K within a pressure range of 12 to 36 MPa using a dynamic method. Experimental solubilities were then correlated using different semi-empirical density based models (Mendez-Santiago and Teja model, Chrastil model, Bartle model, and Kumar and Johnston model) with average absolute relative deviations varying from 6.7 and 11.5% indicating the measurement consistency. As the lowest deviation was obtained with the Kumar and Johnston model (Eq. (1)), this correlation was used to estimate gatifloxacin solubility in supercritical CO_2 under pressures varying from 8 to 25 MPa at 308, 318 and 328 K.

$$\ln y_{GTX} = 3.0100 - \frac{7472.5661}{T} + 0.0070\rho \quad (1)$$

T is the temperature (K) and ρ is the density of $scCO_2$ ($g{\cdot}L^{-1}$) calculated using Span et al. equation (Span and Wagner, 1996).

2.3. Fourier transform infrared micro-spectroscopy (FTIR)

An original experimental set-up combining a FTIR microscope and high-pressure cell was used in this study to simultaneously measure *in-situ* CO_2 sorption within the polymer IOLs and their subsequent swelling (Dubois et al., 2018). The infrared microscope (Perkin-Elmer spotlight 200) operates in a transflection mode and covers a spectral range over 800–6500 cm^{-1} with a resolution of 4 cm^{-1} obtained after the Fourier transformation of 100 accumulated interferograms. The stainless-steel high-pressure cell is equipped with a 12 mm diameter sapphire window and a polished stainless-steel mirror. The IOL (without the haptics) was maintained facing the sapphire window and supported at its center by the mirror as illustrated in Fig. 2. The high-pressure cell withstands pressure up to 40 MPa and temperature up to 473 K. In order to regulate the temperature, a thermocouple is located near a cartridge heater and a second thermocouple is placed close to the sample area to measure the sample temperature with a 1 K accuracy. The cell is connected through a capillary to a hydraulic pressurization system allowing a pressure increase with a standard uncertainty of 0.1 MPa.

The experiments were performed under isothermal conditions, without drugs. In the first step, the spectra of raw IOL (before exposure to CO_2) were recorded. The cell was then filled with CO_2 respecting similar pressurization rates to those used in impregnation experiments. The spectra were measured every 2–5 min during the pressurization phase and recording was then pursued until the thermodynamic equilibrium of CO_2 sorption within the IOL was reached.

An example of the infrared spectra in the wave number range from 3400 to 6500 cm^{-1} of raw IOL as well as IOL exposed to $scCO_2$ at 8 MPa and 35 °C are illustrated in Fig. 3.

Considering the thickness of the IOL (~1 mm), the spectral ranges below 3800 cm^{-1} were saturated. Two band ranges corresponding to the C—H combination modes and overtones of the polymer appear at 3800–4800 cm^{-1} and 5500–6075 cm^{-1}, respectively. During exposure to $scCO_2$, the intensity of the bands corresponding to the polymer decreases, indicating swelling phenomena, whereas two characteristic peaks of CO_2 appear at 4950 and 5070 cm^{-1} indicating the sorption of CO_2 within the polymer. The peak at 4950 cm^{-1} corresponds to the combination mode $\nu_1 + 2\nu_2 + \nu_3$ of CO_2, whereas the peak at 5070 cm^{-1} is assigned to the combination mode $2\nu_1 + \nu_3$. For quantitative measurements, as the peak intensity was higher at 4090 cm^{-1}, this wavenumber was rather used in order to determine CO_2 sorption within the polymer. As peak position and bandwidth of combination bands are expected to be more sensitive to pressure than overtones, the peak range of 5500–6000 cm^{-1} was selected and its area integrated to quantify the polymer swelling.

The concentration of the CO_2 sorbed into the IOL was determined using the Beer-Lambert law applied to CO_2 peak.

$$A_{CO2} = \varepsilon{\cdot}l{\cdot}C_{CO2}. \quad (2)$$

where A_{CO2} is the absorbance at 4950 cm^{-1}, l the path length (cm) equal to twice the IOL's thickness, C_{CO2} the CO_2 concentration ($mol{\cdot}L^{-1}$) and ε the molar extinction coefficient ($L{\cdot}mol^{-1}{\cdot}cm^{-1}$) equal to 0.25 $L{\cdot}mol^{-1}{\cdot}cm^{-1}$ at 4950 cm^{-1}. (Dubois et al., 2018)

As previously described by Kazarian et al. (Flichy et al., 2002;

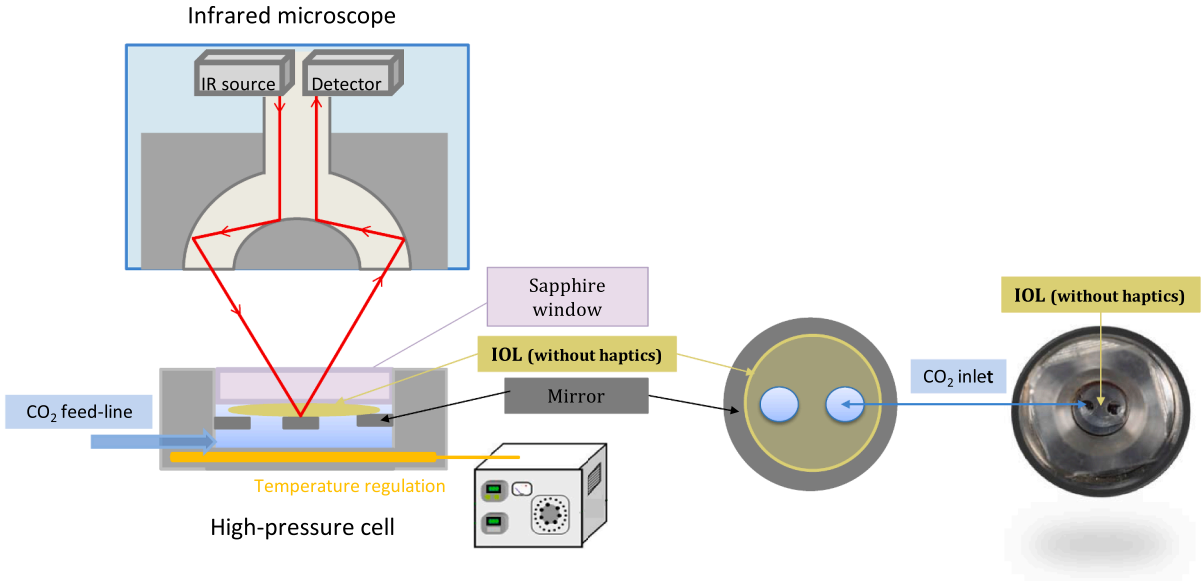

Fig. 2. *In situ* FTIR spectrometer coupled with a transflection high-pressure cell.

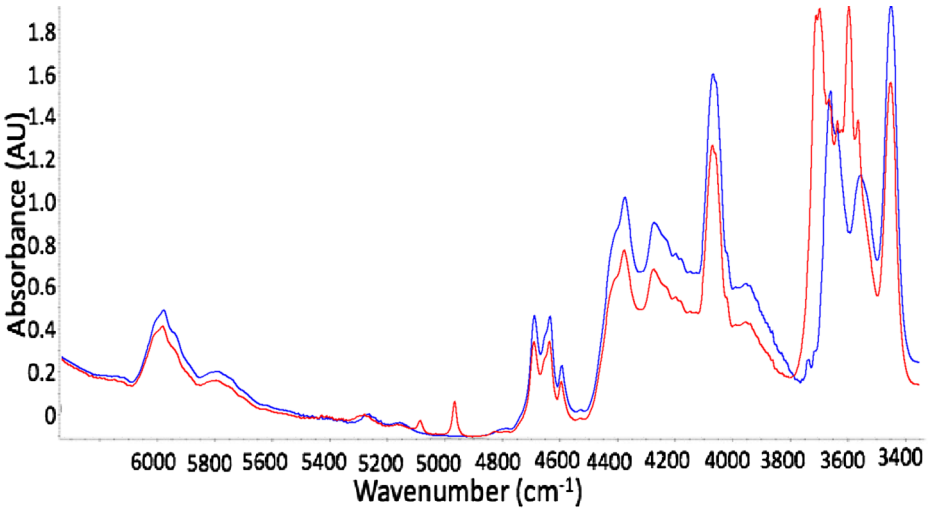

Fig. 3. *In situ* IR spectra of raw IOLs (blue line) and IOLs exposed to $scCO_2$ at 8 MPa and 35 °C after 200 min (Red line). (For interpretation of the references to colour in this figure legend, the reader is referred to the web version of this article.)

Guadagno and Kazarian, 2004), the polymer volume swelling can be calculated using the absorbance of a polymer specific band before and during exposure to CO_2. The absorbance (A) at a specific band can also be calculated following the Beer-Lambert law:

$$A = \varepsilon \cdot l \cdot C_{polymer} \quad (3)$$

$C_{polymer}$ is the polymer concentration ($mol \cdot L^{-1}$) in the IOL, l is the pathlength (twice the IOL thickness in transflection mode) and ε the molar extinction coefficient of the polymer band ($L \cdot mol^{-1} \cdot cm^{-1}$).

ε can be considered to be independent of CO_2 pressure (Dubois et al., 2018) and l is constant since the IOL was maintained between the sapphire window and the mirror.

The absorbance before and during exposure to CO_2 (A_0 and A) can be expressed as follows:

$$A_0 = \varepsilon \cdot l \cdot C_{0polymer} \quad (4)$$

$$A = \varepsilon \cdot l \cdot C_{polymer} \quad (5)$$

where $C_{0polymer}$ and $C_{polymer}$ are respectively the polymer concentration in IOL before and during exposure to CO_2 ($mol \cdot L^{-1}$). If V_0 is the volume occupied by polymer before exposure to CO_2, then the volume during exposure to CO_2 can be expressed as $V_0 + \Delta V$. As the polymer mass does not change during exposure to CO_2, it is possible to write that:

$$\frac{A_0}{A} = \frac{C_{0polymer}}{C_{polymer}} = \frac{V_0 + \Delta V}{V_0} \quad (6)$$

Consequently, the polymer swelling (S) can be expressed as:

$$S = \frac{\Delta V}{V_0}\frac{C_{0polymer}}{C_{polymer}} - 1 = \frac{A_0}{A} - 1 \quad (7)$$

The Beer-Lambert law can also be applied to the integrated absorbance of the polymer between 5500 and 6000 cm^{-1} (Guadagno and Kazarian, 2004).

$$AA_{IOL} = \int_{5500}^{6000} A(\lambda)d\lambda \quad (8)$$

The polymer swelling (S) can therefore be expressed as:

$$S = \frac{AA_{0IOL}}{AA_{IOL}} - 1 \quad (9)$$

2.4. Supercritical impregnation

Supercritical impregnations were conducted in batch mode using a high-pressure set-up and following the experimental protocol described previously (Bouledjouidja et al., 2016, 2017a, 2017b; Masmoudi et al., 2011). For all the experiments, one IOL protected by a filter paper was placed on an aluminum support and 5 mg of gatifloxacin was introduced within a frit filter basket to prevent any contamination of the IOL surface in the 125 mL autoclave. Based on previous studies, a constant pressurization flow rate of 250 $g \cdot h^{-1}$ and a depressurization rate of 0.2 $MPa \cdot min^{-1}$ were respected to avoid IOL foaming (Bouledjouidja et al., 2016). The influence of the operating conditions was studied by varying the impregnation pressure, temperature and duration. The impregnation duration corresponds to the contact time between $scCO_2$ and the IOL at a constant pressure (recorded since the end of the pressurization step).

2.5. Impregnation yields

In order to determine impregnation yields, loaded IOLs were soaked at 37 °C under stirring in 3 mL of simulated aqueous humor (pH of 7.2) prepared as described previously (Bouledjouidja et al., 2016). After several weeks of release, aliquots of 0.4 mL were collected and drug concentration quantified at 287 nm using a spectrophotometer (Jenway 6715, UV/VIS). Time-spaced samples were withdrawn to confirm the stability of the concentration indicating a complete drug release. After each analysis, the aliquot was returned to the release vessel to maintain the initial volume. The impregnation yield (Y_{imp}) was calculated according to Eq. (10).

$$Y_{imp} = \frac{m_{imp}}{m_{0IOL}} \quad (10)$$

where m_{0IOL} is the initial mass of raw IOL and m_{imp} is the drug released mass.

2.6. Partition coefficient

The partition coefficient (K) is defined as the drug concentration in the polymer over its concentration in the fluid phase as indicated in Eq. (11). It highlights the relative affinity of the drug to the polymer towards that of sc CO_2.

$$K = \frac{m_{imp}/m_{0IOL}}{m_{solubilized}/m_{CO_2}} \quad (11)$$

where the $m_{solubilized}/ m_{CO2}$ is the mass ratio of drug solubilized in $scCO_2$ in saturation conditions to $scCO_2$.

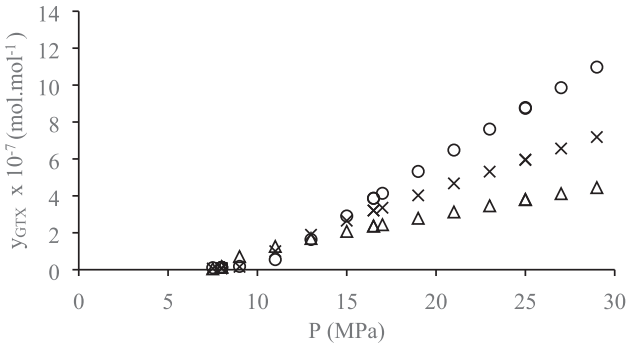

Fig. 4. Gatifloxacin solubility in supercritical CO_2 (y_{GTX}) at (Δ) 308 K, (x) 318 K and (o) 328 K calculated using data from (Shi et al., 2017).

3. Results and discussion

3.1. Solubility of gatifloxacin in supercritical CO_2

The evolution of calculated gatifloxacin solubility in supercritical CO_2 with pressure under isothermal conditions (308, 318 and 328 K) is illustrated in Fig. 4 and shows the presence of a crossover pressure at 14 MPa. Below this pressure, the solubility decreases when the temperature is increased indicating a retrograde solubility. Above 14 MPa, the solubility increases while increasing the temperature. This behavior is explained by two competing effects when the temperature is increased under isobaric conditions. The solute vapor pressure increases, enhancing dissolution phenomena whereas CO_2 density decreases, reducing interactions between solute and CO_2 molecules, thereby limiting the drug dissolution. Below 14 MPa, the effect of the fluid phase density is predominant and retrograde solubility behavior is observed whereas at higher pressures the effect of solute vapor pressure prevails.

3.2. CO_2 sorption and swelling

To study the influence of pressure on CO_2 sorption in the polymer and on the subsequent IOL swelling, FTIR measurements were performed at 308 K and 8 MPa and 25 MPa. For each pressure, CO_2 peak absorbance at 4950 cm^{-1} (A_{CO2}) and integrated area of IOL peaks in the range of 5500–6000 cm^{-1} (AA_{IOL}) were followed *in-situ* and recorded from the supply of the high-pressure cell with CO_2 (including therefore the pressurization step) until thermodynamic equilibrium was reached (Fig. 5). The evolution of corresponding CO_2 concentration within the polymer and the subsequent swelling are illustrated in Fig. 6.

In both experimental conditions, the absorbance of a specific band of CO_2 was negligible during the pressurization step (10 min at 8 MPa and 25 min at 25 MPa) and the integrated area of IOL peaks was constant suggesting negligible sorption of CO_2 within the IOL. During pressurization, as the IOLs support is incompressible and its entangled intrinsic free volume hinders diffusion phenomena, CO_2 is mainly compressed in the free volume of the autoclave and pressure is increased.

When a constant pressure was set within the high-pressure vessel (end of the pressurization step), the absorbance of the CO_2 specific band increased, indicating CO_2 sorption within the polymer until reaching a plateau corresponding to sorption thermodynamic equilibrium (Fig. 5). In the meantime, the integrated area of IOL peaks decreases, implying polymer swelling that stabilizes when sorption thermodynamic equilibrium is reached. The simultaneous evolution of CO_2 sorption and polymer swelling are presented in Fig. 6 and indicate a direct correlation between both phenomena.

The duration required to reach sorption thermodynamic equilibrium (t_{eq}) was defined as the contact time between supercritical CO_2 and the polymer, from pressure stabilization (end of the pressurization step) until reaching constant CO_2 concentration within the polymer. t_{eq} and the corresponding CO_2 concentration and IOL swelling are reported in Table 1. Although one would expect that an increase in pressure from 8 to 25 MPa would significantly increase the CO_2 dissolution in an amorphous polymer, only a slight increase in CO_2 concentration at equilibrium was observed at 25 MPa compared to 8 MPa and the IOL swelling was similar. Such an observation could be explained by the fact that the experiments are performed at a temperature and pressure close to the critical region. The high density fluctuations of CO_2 in this region could explain the high solubility of CO_2 already reached at 8 MPa. A significant reduction in time required for reaching sorption equilibrium at 25 MPa compared to 8 MPa was observed. This difference is also illustrated by a higher slope of CO_2 concentration within the IOL with time at 25 MPa compared to 8 MPa as illustrated in Fig. 7, indicating a faster diffusion kinetic within the IOL at 25 MPa.

3.3. Supercritical impregnation

3.3.1. Experimental repeatability

Supercritical impregnation repeatability was studied by carrying out 4 impregnations at 308 K and 25 MPa (corresponding to a CO_2 density of 902 kg·m^{-3}) for 240 min as presented in Table 2.

In the tested conditions, impregnation yields varied from 0.99 to 1.08 μg·mg$_{IOL}^{-1}$ with an average yield of 1.03 μg·mg$_{IOL}^{-1}$ and a standard deviation of 0.04 μg·mg$_{IOL}^{-1}$ lower than the experimental error and confirming a satisfactory experimental repeatability. These results are in good accordance with previous data obtained with other drug/IOL combinations (Bouledjouidja et al., 2016) (see Table 2).

3.3.2. Influence of operating conditions on supercritical impregnation

The influence of operating conditions on the supercritical

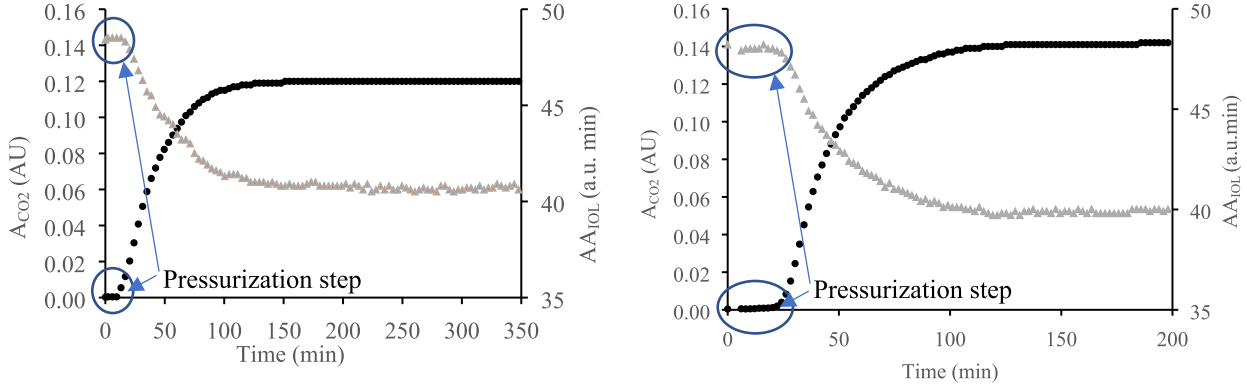

Fig. 5. Evolution of CO_2 peak absorbance at 4950 cm^{-1} (A_{CO2}) (●) and integrated area of IOL peak in the range of 5500–6000 cm^{-1} (AA_{IOL}) (▲) with contact time at 308 K and 8 MPa (left) and 25 MPa (right).

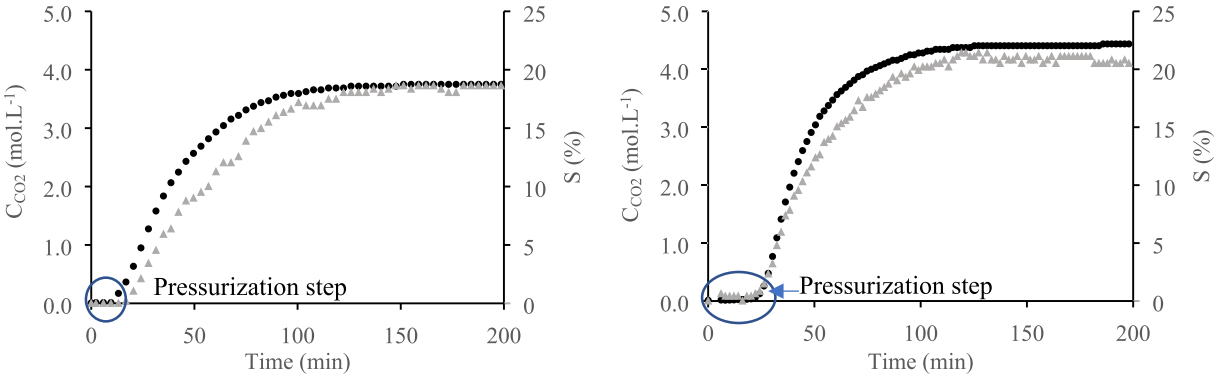

Fig. 6. Evolution of CO_2 concentration (C_{CO2}) (●) and IOL swelling (S%) (▲) with contact time between supercritical CO_2 and IOLs at 308 K and 8 MPa (left) and 25 MPa (right).

Table 1
CO_2 concentration (C_{CO2}) and IOL swelling (S%) determined at sorption thermodynamic equilibrium at 308 K.

Pressure	CO_2 density* ρ_{CO2}	C_{CO2}**	S**	$t_{pressurization}$	t_{eq}**
MPa	kg·m^{-3}	mol.L^{-1}	%	min	min
8	436	3.7	18 ± 2.5	10	95 ± 5
25	902	4.4	20 ± 2.5	25	75 ± 5

* Density data from NIST chemistry webbook using Span and Wagner model (Span and Wagner, 1996).

** Experimental errors: C_{CO2} ± 0.2 mol.L^{-1}; S ± 2.5%; t_{eq} ± 5 min.

Table 2
Repeatability of gatifloxacin impregnation in IOLs at 25 MPa and 308 K for 240 min.

	m_{imp}* µg	Y_{imp}* µg·mg$_{IOL}^{-1}$
	25.1	1.08
	24.6	1.05
	23.1	1.00
	23.0	0.99
Average ± SD	24.0 ± 1.1	1.03 ± 0.04

* Experimental errors: m_{imp} ± 1.2 µg; Y_{imp} ± 0.07 µg·mg$_{IOL}^{-1}$.

impregnation of gatifloxacin into IOLs was studied at 8, 16.5 and 25 MPa. The impregnation temperature and duration were varied from 308 to 328 K and from 30 to 240 min respectively as presented in Table 3. The impregnated masses per IOL (m_{imp}) varied from 7.7 to 24.0 ± 1.2 µg/IOL and impregnation yields (Y_{imp}) from 0.33 to 1.07 ± 0.07 µg·mg$_{IOL}^{-1}$ indicating the influence of the operating conditions on impregnation. All the impregnated IOLs were visually transparent, confirming previous conclusions that controlled pressurization and depressurization conditions prevent the occurrence of foaming phenomena (Bouledjouidja et al., 2016). Based on former works (Bouledjouidja et al., 2017a) and considering the impregnated masses, the optical properties of the IOLs should also be preserved meeting the ISO standards (ISO 11979-2:2014). Indeed, Bouledjouidja et al. impregnated two different active ingredients (ciprofloxacin and dexamethasone 21-phosphate disodium) into hydrophobic and foldable IOLs at 308 K and under 8 and 20 MPa for 2 h. In these conditions, drug impregnated masses varying between 1.8 and 23.7 µg/IOL were obtained and the optical properties of all the impregnated IOls were preserved meeting the ISO standards (ISO 11979-2:2014). As the impregnated masses cover the range obtained within this study in close operating conditions, it can be reasonably hypothesized that the optical properties are maintained.

As illustrated in Fig. 8, supercritical impregnation was promoted with pressure increase from 8 to 25 MPa at the same duration and temperature. Under isothermal conditions, as CO_2 density increases at a higher pressure, its sorption within an amorphous polymer can be expected to be promoted. For the studied IOLs, only a slight increase in CO_2 concentration within the IOLs from 3.7 to 4.4 ± 0.2 mol.L^{-1} was observed when increasing the pressure from 8 to 25 MPa at 308 K and the influence on the subsequent polymer swelling was not significant.

However, gatifloxacin solubility in supercritical CO_2 was greatly enhanced at higher pressures under isothermal conditions. At 308 K, the solubility increases from 0.15 to 3.81 × 10^{-7} mol·mol^{-1} with pressure increase from 8 to 25 MPa and from 0.13 to

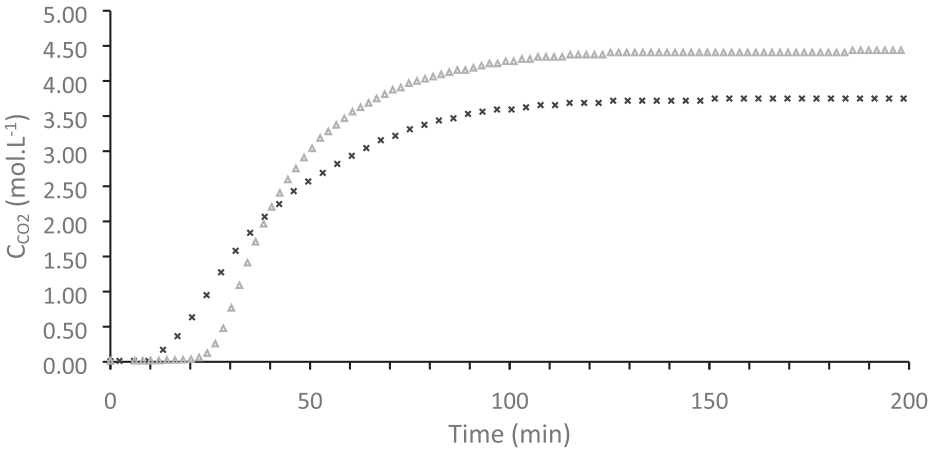

Fig. 7. Evolution of CO_2 concentration (C_{CO2}) with contact time between scCO_2 and IOLs at 308 K and 8 MPa (x) and 25 MPa (▲).

Table 3
Influence of the operating conditions on supercritical impregnation of gatifloxacin into IOLs.

Experiment	P	T	Duration	CO_2 density ρ_{CO2}	y_{GTX} ** ($\times 10^7$)	m_{imp}*	Yimp*
	MPa	K	min	kg·m^{-3}	mol.mol^{-1}	µg	µg·mg$_{IOL}^{-1}$
1	8	308	30	436	0.15 ± 0.01	7.7	0.33
2			240	436	0.15 ± 0.01	11.7	0.51
3		328	30	204	0.13 ± 0.01	10.9	0.47
4			240	204	0.13 ± 0.01	11.5	0.49
5	16.5	318	30	769	3.21 ± 0.21	8.1	0.35
6			240	769	3.21 ± 0.21	22.8	1.05
7		328	135	694	3.87 ± 0.26	22.8	1.07
8	25	308	30	902	3.81 ± 0.26	13.3	0.58
9			240	902	3.81 ± 0.26	24.0	1.03
10		328	30	811	8.78 ± 0.59	20.8	0.90

* Experimental errors: m_{imp} ± 1.2 µg; Y_{imp} ± 0.07 µg·mg$_{IOL}^{-1}$.
** The solubility precision was deteminated by the average relative deviation indicated by Shi et al. (2017).

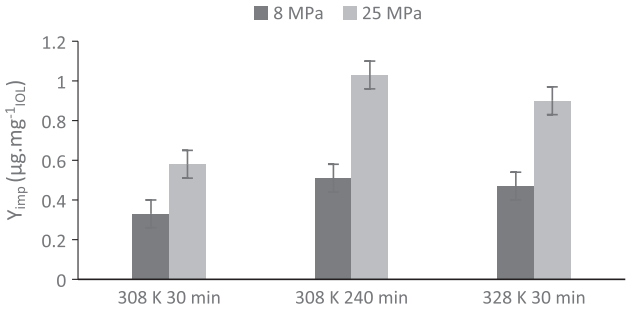

Fig. 8. Influence of pressure on IOL impregnation yield at different experimental conditions.

8.78 × 10^{-7} mol·mol^{-1} at 328 K. The variation of the impregnation yield with the pressure under isothermal conditions is therefore related to the variation of the drug dissolution within the fluid phase rather than to the polymer swelling.

The influence of increasing the temperature from 308 to 328 K at similar impregnation duration and pressure is illustrated in Fig. 9. At 8 MPa, similar impregnation yields are obtained at both temperatures whatever the impregnation duration. However, at 25 MPa, a higher impregnation yield is obtained at 328 K compared to 308 K.

As aforementioned in the solubility discussion part, a crossover pressure of the solubilibity curves is observed at 14 MPa (Fig. 4). At 8 MPa, in the retrograde solubility zone, gatifloxacin solubility in supercritical CO_2 decreases when the temperature is increased from 308 to 328 K. Nevertheless, the variation of the solubility is relatively small (0.15–0.13 × 10^{-7} mol·mol^{-1}) which can explain the similar impregnation yields obtained at 8 MPa.

At 25 MPa, over the crossover pressure, increasing the temperature from 308 to 328 K promotes the drug solubility from 3.81 to 8.78 × 10^{-7} mol·mol^{-1}. Even if one hypothesizes that 30 min could not be enough to reach the gatifloxacin solubilization equilibrium, an increase in drug concentration in the fluid phase should be observed for similar contact duration at higher temperature, thus favoring impregnation.

Under isobaric conditions, diffusion phenomena are enhanced at higher temperatures which also promotes impregnation. Furthermore, in amorphous polymers, increasing the temperature favors the polymer chain mobility above its glass transition temperature (Champeau et al., 2015b) which can further enhance diffusion phenomena. On the other hand, the decrease in CO_2 density at higher temperatures could be expected to be unfavorable towards CO_2 sorption in amorphous polymers. Nevertheless, as already highlighted, the influence of CO_2 density on its sorption into the studied IOLs is low which should not significantly influence impregnation.

In order to study the influence of the duration, impregnations were carried out at similar pressures and temperatures for 30 and 240 min, respectively below and beyond the CO_2 sorption equilibrium duration. Corresponding impregnation yields are compared in pairs in Fig. 10 where the experimental conditions are sorted in order of increasing CO_2 density.

At constant pressure and temperature, supercritical impregnation is enhanced by increasing the duration from 30 to 240 min, in particular at higher CO_2 density conditions. Indeed, at 8 MPa, similar impregnation yields were obtained at 328 K (ρ_{CO2} = 204 kg·m^{-3}) and a slight increase was observed at 308 K (ρ_{CO2} = 436 kg·m^{-3}) when impregnation was extended from 30 to 240 min. At higher CO_2 densities of 769 kg·m^{-3} and 902 kg·m^{-3}, impregnation yields were significantly higher for an impregnation duration of 240 min.

Following the evolution of CO_2 concentration (C_{CO2}) within the polymer IOLs and the subsequent swelling of the latters (Figs. 5 and 6), 30 min is not sufficient to reach CO_2 sorption equilibrium in the studied

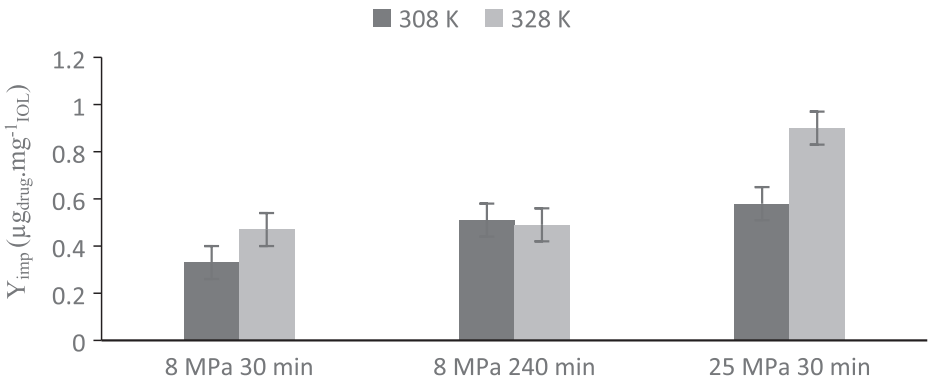

Fig. 9. Influence of temperature on IOL impregnation yield at different experimental conditions.

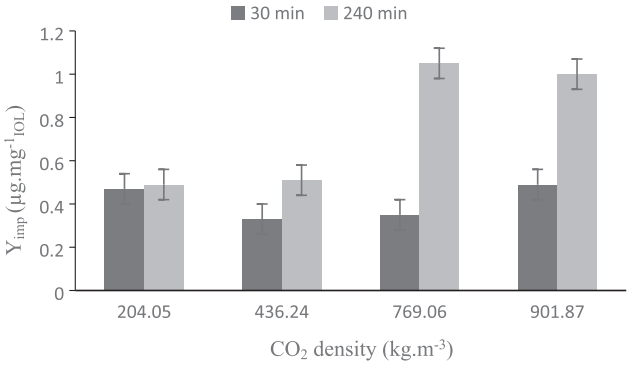

Fig. 10. Influence of impregnation duration on IOL impregnation yield.

conditions whereas at 240 min the CO_2 sorption is complete. The most pronounced enhancement of impregnation with the duration at a higher CO_2 density, could not be explained by CO_2 soprtion kinetic. Indeed, the difference in CO_2 concentration within the IOLs between 30 min and 240 min is lower at higher CO_2 densities as 75% of total CO_2 is sorbed within the IOLs over 30 min at 25 MPa and 308 K (ρ_{CO2} = 902 kg·m^{-3}), compared to 60% at 8 MPa and 308 K (ρ_{CO2} = 436 kg·m^{-3}).

In order to explain this behavior, it could be hypothesized that gatifloxacin solubilization equilibrium is not reached in 30 min. Therefore, as gatifloxacin solubility is enhanced at higher CO_2 densities, even if the difference in CO_2 concentration within the IOLs is lower, as the solubilized gatifloxacin concentration in the fluid phase and therefore carried within the IOLs is significantly higher, the influence of the duration on impregnation is more pronounced. To support this hypothesis, the CO_2 residence times used for solubility measurements in Shi *et al.* work (Shi et al., 2017) were calculated.

The authors used a dynamic method to measure gatifloxacin solubility in supercritical CO_2 and the CO_2 flow rate through a dissolution high pressure cell (32 cm^3) was varied from 18 to 54 mg·min^{-1} at 333 K and 36 MPa to achieve dissolution equilibrium. Gatifloxacin concentration in supercritical CO_2 increased when the flow rate was decreased from 54 to 36 mg·min^{-1} but remained stable when the CO_2 flow rate was further decreased to 18 mg·min^{-1}, indicating that in their studied experimental conditions, a CO_2 residence time comprised between 515 and 773 min is required to reach solubility. Even if these durations cannot be directly transposed in batch mode and at lower conditions of pressure and temperature, they give an indication that gatifloxacin dissolution in supercritical CO_2 could be time-consuming and could therefore be enhanced at a longer duration of 240 min compared to 30 min. As gatifloxacin solubility is significanlty higher at 25 MPa, the difference in drug concentration in the fluid phase when increasing the contact duration could be higher than that at 8 MPa. It should also be emphasized that the drug diffusivity within the IOL could be slower than that of CO_2, which could also explain higher differences in impregnation yields between 8 and 25 MPa at longer durations (Champeau et al., 2015a).

In order to highlight the influence of CO_2 density, the impregnation yields were compared only for impregnation durations longer than 135 min to be in CO_2 sorption equilibrium conditions (see Table 4). As can be observed in Fig. 11, whatever the pressure and the temperature, higher impregnation yields were obtained for higher solubilities. In the studied conditions, an impregnation yield of almost 1 µg·mg$^{-1}_{IOL}$ was obtained for solubility varying between 3.21 and 3.87 × 10^{-7} mol·mol^{-1}, whereas only about 0.5 µg·mg$^{-1}_{IOL}$ was obtained at lower solubilities of 0.13 and 0.15 × 10^{-7} mol·mol^{-1}.

When comparing the partition coefficients (see Table 4), in spite of an impregnation enhancement for higher drug solubilities in supercritical CO_2, a significant decrease in the partition coefficient was observed from 4085 to 4593 to 318–383. This variation is explained by an increase in the drug solubility up to 30 fold that outweighs that of the impregnation yield which was doubled.

4. Conclusions

Gatifloxacin, a bactericidal antibiotic of fourth-generation fluoroquinolones, was loaded into commercially available hydrophobic foldable IOLs for the elaboration of drug delivery systems for the prevention of endophthalmitis. For that purpose, the supercritical CO_2 impregnation process was carried out in batch mode while varying the operating conditions of pressure (8–25 MPa), temperature (308–328 K) and impregnation durations (30–240 min). Effective impregnations varying from 0.33 to 1.07 ± 0.07 µg·mg$^{-1}_{IOL}$ were obtained. In order to explain the impregnation yield evolution, different phenomena involved in supercritical impregnation were investigated. Gatifloxacin solubility in supercritical CO_2 was calculated from the literature data using a validated density-based semi-emprical (Kumar and Johnston) model (Shi et al., 2017). Solubility evolution shows a crossover pressure corresponding to the upper limit of the retrograde solubility zone at 14 MPa.

CO_2 sorption within the IOLs and the subsequent IOL swelling were followed *in-situ* through Fourier transform infrared micro-spectroscopy (FTIR). At 308 K, the duration necessary to reach CO_2 sorption equilibrium varies between 75 and 95 min after a pressure stabilization respectively at 25 and 8 MPa. Even if CO_2 concentration was only slightly enhanced at higher pressure and the subsequent polymer swelling not significantly increased, the diffusion kinetic was enhanced.

The variation of the impregnation duration below and beyond CO_2 sorption equilibrium time was shown to have a more significant influence at high CO_2 density conditions (769 and 902 kg·m^{-3} compared to 204 and 436 kg·m^{-3}), explained by a higher gatifloxacin solubility in supercritical CO_2, which should imply larger variations on drug concentration in the fluid phase with the duration if thermodynamic dissolution is not reached. At long impregnation durations sufficient to establish CO_2 sorption equilibrium, higher drug solubility conditions in supercritical CO_2 were favorable for enhancing impregnation for the studied drug/IOL components.

CRediT authorship contribution statement

Kanjana Ongkasin: Formal analysis, Validation, Investigation, Writing - original draft. **Yasmine Masmoudi:** Conceptualization,

Table 4
Partition coefficients of gatifloxacin between the IOLs and the fluid phase in CO_2 sorption equilibrium conditions.

Experiment	P	T	Duration	CO_2 density ρ_{CO2}	y_{GTX} (×10^7)	Yimp ± 0.07	Partition coefficient K
	MPa	K	min	kg·m^{-3}	mol.mol^{-1}	µg·mg$^{-1}_{IOL}$	
2	8	308	240	436	0.15 ± 0.01	0.51	4085
4		328	240	204	0.13 ± 0.01	0.49	4593
6	16.5	318	240	769	3.21 ± 0.21	1.05	383
7		328	135	694	3.87 ± 0.26	1.07	324
9	25	308	240	902	3.81 ± 0.26	1.03	318

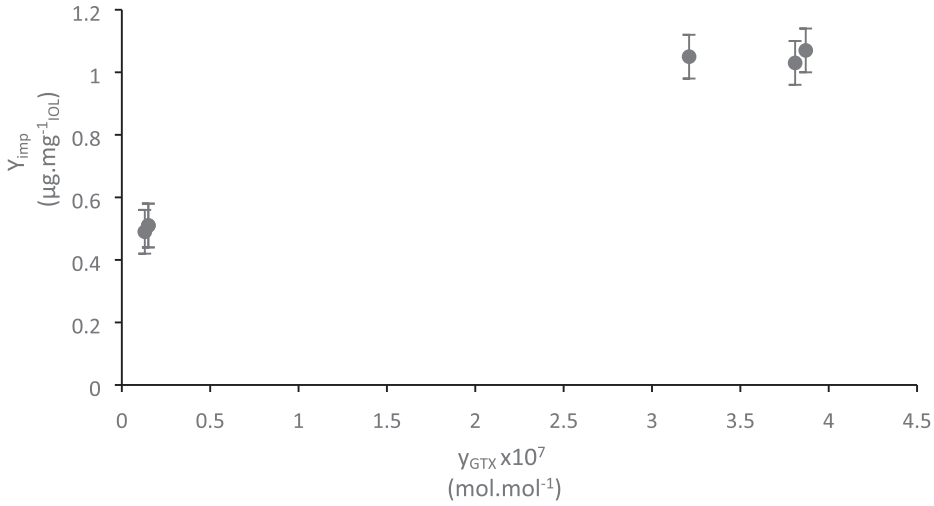

Fig. 11. Evolution of impregnation yields (Y_{imp}) with gatifloxacin solubility in supercritical CO_2 (y_{GTX}).

Methodology, Supervision, Resources, Writing - review & editing, Project administration. **Thierry Tassaing:** Conceptualization, Methodology, Supervision. **Gwenaelle Le-Bourdon:** Formal analysis, Investigation. **Elisabeth Badens:** Conceptualization, Methodology, Supervision, Resources, Writing - review & editing, Project administration, Funding acquisition.

Declaration of Competing Interest

The authors declare that they have no known competing financial interests or personal relationships that could have appeared to influence the work reported in this paper.

Acknowledgements

The authors would like to thank the Thai Ministry of Science and Technology for providing the Royal Thai Government Scholarship to support the PhD thesis of Kanjana Ongkasin.

Shenyang Bio Medical Device Co. Ltd. and He eye care system (Liaoning Province, China) are also acknowledged for kindly providing the intraocular lenses used within this study.

References

Alhusban, Ala A., Tarawneh, O.A., Dawabsheh, S.O., Alhusban, Ahmad A., Abumhareb, F.W., 2019. Liquid chromatography–tandem mass spectrometry for rapid and selective simultaneous determination of fluoroquinolones level in human aqueous humor. J. Pharmacol. Toxicol. Methods 97, 36–43. https://doi.org/10.1016/j.vascn.2019.03.001.

Arantes, T.E.F.E., Castro, C.M.M.B. de, Cavalcanti, R.F., Severo, M.S., Diniz, M. de F.A., Urtiga, R.W. de D., 2008. [Conjunctival bacterial flora after topical use of ciprofloxacin and gatifloxacin in cataract surgery]. Arq. Bras. Oftalmol. 71, 191–196. Doi: 10.1590/S0004-27492008000200012.

Badens, E., Masmoudi, Y., Mouahid, A., Crampon, C., 2018. Current situation and perspectives in drug formulation by using supercritical fluid technology. J. Supercrit. Fluids 134, 274–283. https://doi.org/10.1016/j.supflu.2017.12.038.

Barros, A.A., Silva, J.M., Craveiro, R., Paiva, A., Reis, R.L., Duarte, A.R.C., 2017. Green solvents for enhanced impregnation processes in biomedicine. Curr. Opin. Green Sustain. Chem. 5, 82–87. https://doi.org/10.1016/j.cogsc.2017.03.014.

Bouledjouidja, A., Masmoudi, Y., Li, Y., He, W., Badens, E., 2017a. Supercritical impregnation and optical characterization of loaded foldable intraocular lenses using supercritical fluids. J. Cataract Refract. Surg. 43, 1343–1349. https://doi.org/10.1016/j.jcrs.2017.07.033.

Bouledjouidja, A., Masmoudi, Y., Sergent, M., Badens, E., 2017b. Effect of operational conditions on the supercritical carbon dioxide impregnation of anti-inflammatory and antibiotic drugs in rigid commercial intraocular lenses. J. Supercrit. Fluids 130, 63–75. https://doi.org/10.1016/j.supflu.2017.07.015.

Bouledjouidja, A., Masmoudi, Y., Sergent, M., Trivedi, V., Meniai, A., Badens, E., 2016. Drug loading of foldable commercial intraocular lenses using supercritical impregnation. Int. J. Pharm. 500, 85–99. https://doi.org/10.1016/j.ijpharm.2016.01.016.

Braga, M.E.M., Costa, V.P., Pereira, M.J.T., Fiadeiro, P.T., Gomes, A.P.A.R., Duarte, C.M.M., de Sousa, H.C., 2011. Effects of operational conditions on the supercritical solvent impregnation of acetazolamide in Balafilcon A commercial contact lenses. Int. J. Pharm. 420, 231–243. https://doi.org/10.1016/j.ijpharm.2011.08.040.

Champeau, M., Thomassin, J.M., Jérôme, C., Tassaing, T., 2015a. In situ investigation of supercritical CO_2 assisted impregnation of drugs into a polymer by high pressure FTIR micro-spectroscopy. The Analyst 140, 869–879. https://doi.org/10.1039/C4AN01130A.

Champeau, M., Thomassin, J.M., Tassaing, T., Jérôme, C., 2015b. Drug loading of polymer implants by supercritical CO_2 assisted impregnation: A review. J. Controlled Release 209, 248–259. https://doi.org/10.1016/j.jconrel.2015.05.002.

Chang, D.F., Braga-Mele, R., Henderson, B.A., Mamalis, N., Vasavada, A., 2015. Antibiotic prophylaxis of postoperative endophthalmitis after cataract surgery: Results of the 2014 ASCRS member survey. J. Cataract Refract. Surg. 41, 1300–1305. https://doi.org/10.1016/j.jcrs.2015.01.014.

Costa, V.P., Braga, M.E.M., Duarte, C.M.M., Alvarez-Lorenzo, C., Concheiro, A., Gil, M.H., de Sousa, H.C., 2010. Anti-glaucoma drug-loaded contact lenses prepared using supercritical solvent impregnation. J. Supercrit. Fluids 53, 165–173. https://doi.org/10.1016/j.supflu.2010.02.007.

Danion, A., Arsenault, I., Vermette, P., 2007a. Antibacterial activity of contact lenses bearing surface-immobilized layers of intact liposomes loaded with levofloxacin. J. Pharm. Sci. 96, 2350–2363. https://doi.org/10.1002/jps.20871.

Danion, A., Brochu, H., Martin, Y., Vermette, P., 2007b. Fabrication and characterization of contact lenses bearing surface-immobilized layers of intact liposomes. J. Biomed. Mater. Res. A 82A, 41–51. https://doi.org/10.1002/jbm.a.31147.

Danion, A., Doillon, C.J., Giasson, C.J., Djouahra, S., Sauvageau, P., Paradis, R., Vermette, P., 2007c. Biocompatibility and light transmission of liposomal lenses: optom. Vis. Sci. 84, 954–961. https://doi.org/10.1097/OPX.0b013e318157a6d5.

Das, T., Sharma, S., 2018. Endophthalmitis prevention. Asia-Pac. J. Ophthalmol. 7, 69–71. https://doi.org/10.22608/APO.201866.

Davies, O.R., Lewis, A.L., Whitaker, M.J., Tai, H., Shakesheff, K.M., Howdle, S.M., 2008. Applications of supercritical CO_2 in the fabrication of polymer systems for drug delivery and tissue engineering. Adv. Drug Deliv. Rev. 60, 373–387. https://doi.org/10.1016/j.addr.2006.12.001.

Dias, A.M.A., Braga, M.E.M., Seabra, I.J., Ferreira, P., Gil, M.H., de Sousa, H.C., 2011. Development of natural-based wound dressings impregnated with bioactive compounds and using supercritical carbon dioxide. Int. J. Pharm. 408, 9–19. https://doi.org/10.1016/j.ijpharm.2011.01.063.

Duarte, A.R.C., Mano, J.F., Reis, R.L., 2009. Supercritical fluids in biomedical and tissue engineering applications: a review. Int. Mater. Rev. 54, 214–222. https://doi.org/10.1179/174328009X411181.

Duarte, A.R.C., Simplicio, A.L., Vega-González, A., Subra-Paternault, P., Coimbra, P., Gil, M.H., de Sousa, H.C., Duarte, C.M.M., 2008. Impregnation of an intraocular lens for ophthalmic drug delivery. Curr. Drug Deliv. 5, 102–107. https://doi.org/10.2174/156720108783954851.

Duarte, A.R.C., Simplicio, A.L., Vega-González, A., Subra-Paternault, P., Coimbra, P., Gil, M.H., de Sousa, H.C., Duarte, C.M.M., 2007. Supercritical fluid impregnation of a biocompatible polymer for ophthalmic drug delivery. J. Supercrit. Fluids 42, 373–377. https://doi.org/10.1016/j.supflu.2007.01.007.

Dubois, J., Grau, E., Tassaing, T., Dumon, M., 2018. On the CO_2 sorption and swelling of elastomers by supercritical CO_2 as studied by in situ high pressure FTIR microscopy. J. Supercrit. Fluids 131, 150–156. https://doi.org/10.1016/j.supflu.2017.09.003.

Eibl, K.H., Wertheimer, C., Kernt, M., Wolf, A., Kook, D., Haritoglou, C., Kampik, A., 2013. Alkylphosphocholines for intraocular lens coating. J. Cataract Refract. Surg. 39, 438–445. https://doi.org/10.1016/j.jcrs.2012.09.028.

Findl, O., 2009. Intraocular lens materials and design. In: Michael Colvard, D. (Ed.), Achieving Excellence in Cataract Surgery – A Step-by-step Approach.

Flaxman, S.R., et al., 2017. Global causes of blindness and distance vision impairment 1990–2020: a systematic review and meta-analysis. Lancet Glob. Health 5, e1221–e1234. https://doi.org/10.1016/S2214-109X(17)30393-5.

Fleming, O.S., Kazarian, S.G., 2005. Polymer processing with supercritical fluids. Supercrit. Carbon Dioxide Polym. React. Eng. 205–238. https://doi.org/10.1002/3527606726.ch10.

Flichy, N.M.B., Kazarian, S.G., Lawrence, C.J., Briscoe, B.J., 2002. An ATR−IR study of poly(dimethylsiloxane) under high-pressure carbon dioxide: simultaneous measurement of sorption and swelling. J. Phys. Chem. B 106, 754–759. https://doi.org/10.1021/jp012597q.

Garg, P., Roy, A., Sharma, S., 2017. Endophthalmitis after cataract surgery: epidemiology, risk factors, and evidence on protection. Curr. Opin. Ophthalmol. 28, 67–72. https://doi.org/10.1097/ICU.0000000000000326.

Gerber, C.M., 2000. Grepafloxacin against penicillin-resistant pneumococci in the rabbit meningitis model. J. Antimicrob. Chemother. 46, 249–253. https://doi.org/10.1093/jac/46.2.249.

Guadagno, T., Kazarian, S.G., 2004. High-pressure CO_2 –expanded solvents: simultaneous measurement of CO_2 sorption and swelling of liquid polymers with in-situ near-IR spectroscopy. J. Phys. Chem. B 108, 13995–13999. https://doi.org/10.1021/jp0481097.

Gulsen, D., Chauhan, A., 2005. Dispersion of microemulsion drops in HEMA hydrogel: a potential ophthalmic drug delivery vehicle. Int. J. Pharm. 292, 95–117. https://doi.org/10.1016/j.ijpharm.2004.11.033.

Gulsen, D., Chauhan, A., 2004. Ophthalmic drug delivery through contact lenses. Investig. Opthalmol. Vis. Sci. 45, 2342. https://doi.org/10.1167/iovs.03-0959.

Hiratani, H., Fujiwara, A., Tamiya, Y., Mizutani, Y., Alvarez-Lorenzo, C., 2005. Ocular release of timolol from molecularly imprinted soft contact lenses. Biomaterials 26, 1293–1298. https://doi.org/10.1016/j.biomaterials.2004.04.030.

Jain, R., Shastri, J., 2011. Study of ocular drug delivery system using drug-loaded liposomes. Int. J. Pharm. Investig. 1, 35. https://doi.org/10.4103/2230-973X.76727.

Javitt, J.C., 2016. Intracameral antibiotics reduce the risk of endophthalmitis after cataract surgery: does the preponderance of the evidence mandate a global change in practice? Ophthalmology 123, 226–231. https://doi.org/10.1016/j.ophtha.2015.12.011.

Jensen, M.K., Fiscella, R.G., Moshirfar, M., Mooney, B., 2008. Third- and fourth-generation fluoroquinolones: retrospective comparison of endophthalmitis after cataract surgery performed over 10 years. J. Cataract Refract. Surg. 34, 1460–1467. https://doi.org/10.1016/j.jcrs.2008.05.045.

Jung, H.J., Abou-Jaoude, M., Carbia, B.E., Plummer, C., Chauhan, A., 2013. Glaucoma therapy by extended release of timolol from nanoparticle loaded silicone-hydrogel contact lenses. J. Controlled Release 165, 82–89. https://doi.org/10.1016/j.jconrel.2012.10.010.

Kapoor, Y., Thomas, J.C., Tan, G., John, V.T., Chauhan, A., 2009. Surfactant-laden soft contact lenses for extended delivery of ophthalmic drugs. Biomaterials 30, 867–878. https://doi.org/10.1016/j.biomaterials.2008.10.032.

Kazarian, S., 2004. Supercritical fluid impregnation of polymers for drug delivery. In: York, P., Kompella, U., Shekunov, B. (Eds.), Supercritical Fluid Technology for Drug Product Development. Informa Healthcare.

Kazarian, S.G., 2000. Polymer processing with supercritical fluids. Polym. Sci. 42, 78–101220.

Kazarian, S.G., Vincent, M.F., West, B.L., Eckert, C.A., 1998. Partitioning of solutes and cosolvents between supercritical CO_2 and polymer phases. J. Supercrit. Fluids 13, 107–112. https://doi.org/10.1016/S0896-8446(98)00041-2.

Kernt, M., Kampik, A., 2010. Endophthalmitis: pathogenesis, clinical presentation, management, and perspectives. Clin. Ophthalmol. Auckl. NZ 4, 121–135. https://doi.org/10.2147/opth.s6461.

Kikic, I., Vecchione, F., 2003. Supercritical impregnation of polymers. Curr. Opin. Solid State Mater. Sci. 7, 399–405. https://doi.org/10.1016/j.cossms.2003.09.001.

Kohnen, T., Koch, D.D., 2005. Cataract and Refractive Surgery. Springer-Verlag Berlin Heidelberg, Berlin, Heidelberg.

Kugelberg, M., Shafiei, K., van der Ploeg, I., Zetterström, C., 2010. Intraocular lens as a drug delivery system for dexamethasone. Acta Ophthalmol. (Copenh.) 88, 241–244. https://doi.org/10.1111/j.1755-3768.2008.01419.x.

Li, C.C., Abrahamson, M., Kapoor, Y., Chauhan, A., 2007. Timolol transport from microemulsions trapped in HEMA gels. J. Colloid Interface Sci. 315, 297–306. https://doi.org/10.1016/j.jcis.2007.06.054.

Li, C.C., Chauhan, A., 2006. Modeling Ophthalmic Drug Delivery by Soaked Contact Lenses. Ind. Eng. Chem. Res. 45, 3718–3734. https://doi.org/10.1021/ie0507934.

Masmoudi, Y., Ben Azzouk, L., Forzano, O., Andre, J.M., Badens, E., 2011. Supercritical impregnation of intraocular lenses. J. Supercrit. Fluids 60, 98–105. https://doi.org/10.1016/j.supflu.2011.08.014.

Matos, R.L., Vieira de Melo, S.A.B., Cabral Albuquerque, E.C.M., Foster, N.R., 2019. Dense CO_2 technology: overview of recent applications for drug processing/formulation/delivery. Chem. Eng. Process. – Process Intensif. 140, 64–77. https://doi.org/10.1016/j.cep.2019.04.009.

Matsushima, H., Mukai, K., Gotoo, N., Yoshida, S., Yoshida, T., Sawano, M., Senoo, T., Obara, Y., Clark, J.I., 2005. The effects of drug delivery via hydrophilic acrylic (hydrogel) intraocular lens systems on the epithelial cells in culture. Ophthal. Surg. Lasers Imag. Off J. Int. Soc. Imag. Eye 36, 386–392. https://doi.org/10.3928/1542-8877-20050901-07.

Maulvi, F.A., Patil, R.J., Desai, A.R., Shukla, M.R., Vaidya, R.J., Ranch, K.M., Vyas, B.A., Shah, S.A., Shah, D.O., 2019. Effect of gold nanoparticles on timolol uptake and its release kinetics from contact lenses: In vitro and in vivo evaluation. Acta Biomater. 86, 350–362. https://doi.org/10.1016/j.actbio.2019.01.004.

Mehta, P., Al-Kinani, A.A., Arshad, M.S., Chang, M.-W., Alany, R.G., Ahmad, Z., 2017. Development and characterisation of electrospun timolol maleate-loaded polymeric contact lens coatings containing various permeation enhancers. Int. J. Pharm. 532, 408–420. https://doi.org/10.1016/j.ijpharm.2017.09.029.

Miller, D., 2006. In vitro fluoroquinolone resistance in staphylococcal endophthalmitis isolates. Arch. Ophthalmol. 124, 479. https://doi.org/10.1001/archopht.124.4.479.

Pasquali, I., Bettini, R., 2008. Are pharmaceutics really going supercritical? Int. J. Pharm. 364, 176–187. https://doi.org/10.1016/j.ijpharm.2008.05.014.

Perrig, M., Acosta, F., Cottagnoud, M., Gerber, C.M., Tauber, M.G., Cottagnoud, P., 2001. Efficacy of gatifloxacin alone and in combination with cefepime against penicillin-resistant Streptococcus pneumoniae in a rabbit meningitis model and in vitro. J. Antimicrob. Chemother. 47, 701–704. https://doi.org/10.1093/jac/47.5.701.

Phan, C.-M., Bajgrowicz-Cieslak, M., Subbaraman, L.N., Jones, L., 2016. Release of moxifloxacin from contact lenses using an in vitro eye model: impact of artificial tear fluid composition and mechanical rubbing. Transl. Vis. Sci. Technol. 5, 3. https://doi.org/10.1167/tvst.5.6.3.

Rengaraj, V., Ma, S.S., Chang, D.F., 2016. Manual small-incision cataract surgery. In: Henderson, B.A. (Ed.), Manual Small Incision Cataract Surgery. Springer International Publishing, Cham, pp. 1–15. https://doi.org/10.1007/978-3-319-24666-6_1.

Ribeiro, A., Veiga, F., Santos, D., Torres-Labandeira, J.J., Concheiro, A., Alvarez-Lorenzo, C., 2012. Hydrophilic acrylic hydrogels with built-in or pendant cyclodextrins for delivery of anti-glaucoma drugs. Carbohydr. Polym. 88, 977–985. https://doi.org/10.1016/j.carbpol.2012.01.053.

Rodoni, D., Hänni, F., Gerber, C.M., Cottagnoud, M., Neftel, K., Täuber, M.G., Cottagnoud, P., 1999. Trovafloxacin in combination with vancomycin against penicillin-resistant pneumococci in the rabbit meningitis model. Antimicrob. Agents Chemother. 43, 963–965. https://doi.org/10.1128/AAC.43.4.963.

Rodriguez-Tenreiro, C., Alvarez-Lorenzo, C., Rodriguez-Perez, A., Concheiro, A., Torres-Labandeira, J.J., 2006. New cyclodextrin hydrogels cross-linked with diglycidylethers with a high drug loading and controlled release ability. Pharm. Res. 23, 121–130. https://doi.org/10.1007/s11095-005-8924-y.

Schultz, C., 2012. Gatifloxacin ophthalmic solution for treatment of bacterial conjunctivitis: safety, efficacy and patient perspective. Ophthalmol. Eye Dis. 4, OED.S7383. https://doi.org/10.4137/OED.S7383.

Shi, K., Feng, L., He, L., Li, H., 2017. Solubility determination and correlation of gatifloxacin, enrofloxacin, and ciprofloxacin in supercritical CO_2. J. Chem. Eng. Data 62, 4235–4243. https://doi.org/10.1021/acs.jced.7b00601.

Soares, G.C., Learmonth, D.A., Vallejo, M.C., Davila, S.P., González, P., Sousa, R.A., Oliveira, A.L., 2019. Supercritical CO_2 technology: the next standard sterilization technique? Mater. Sci. Eng. C 99, 520–540. https://doi.org/10.1016/j.msec.2019.01.121.

Span, R., Wagner, W., 1996. A new equation of state for carbon dioxide covering the fluid region from the triple-point temperature to 1100 K at pressures up to 800 MPa. J. Phys. Chem. Ref. Data 25, 1509–1596. https://doi.org/10.1063/1.555991.

Topete, A., Oliveira, A.S., Fernandes, A., Nunes, T.G., Serro, A.P., Saramago, B., 2018. Improving sustained drug delivery from ophthalmic lens materials through the control of temperature and time of loading. Eur. J. Pharm. Sci. 117, 107–117. https://doi.org/10.1016/j.ejps.2018.02.017.

Üzer, S., Akman, U., Hortaçsu, Ö., 2006. Polymer swelling and impregnation using supercritical CO_2: a model-component study towards producing controlled-release drugs. J. Supercrit. Fluids 38, 119–128. https://doi.org/10.1016/j.supflu.2005.11.005.

Varadaraj, V., Khanna, R.C., Congdon, N., 2019. Innovative approaches in the delivery of eye care: cataract. In: Khanna, R.C., Rao, G.N., Marmamula, S. (Eds.), Innovative Approaches in the Delivery of Primary and Secondary Eye Care. Springer International Publishing, Cham, pp. 107–125. https://doi.org/10.1007/978-3-319-98014-0_8.

Wang, B., Lin, Q., Jin, T., Shen, C., Tang, J., Han, Y., Chen, H., 2015. Surface modification of intraocular lenses with hyaluronic acid and lysozyme for the prevention of endophthalmitis and posterior capsule opacification. RSC Adv. 5, 3597–3604. https://doi.org/10.1039/C4RA13499K.

Weidner, E., 2018. Impregnation via supercritical CO_2 – What we know and what we need to know. J. Supercrit. Fluids 134, 220–227. https://doi.org/10.1016/j.supflu.2017.12.024.

Wertheimer, C., Liegl, R., Wolf, A.H., Kampik, A., Eibl-Lindner, K.H., 2015. Erufosine coated hydrophilic intraocular lenses attenuate PCO formation in vitro. J. Clin. Exp. Ophthalmol. 06. https://doi.org/10.4172/2155-9570.1000453.

Yokozaki, Y., Sakabe, J., Ng, B., Shimoyama, Y., 2015a. Effect of temperature, pressure and depressurization rate on release profile of salicylic acid from contact lenses prepared by supercritical carbon dioxide impregnation. Chem. Eng. Res. Des. 100, 89–94. https://doi.org/10.1016/j.cherd.2015.05.008.

Yokozaki, Y., Sakabe, J., Shimoyama, Y., 2015b. Enhanced impregnation of hydrogel contact lenses with salicylic acid by addition of water in supercritical carbon dioxide. Chem. Eng. Res. Des. 104, 203–207. https://doi.org/10.1016/j.cherd.2015.08.007.

Yokozaki, Y., Shimoyama, Y., 2018. Loading of vitamin E into silicone hydrogel by supercritical carbon dioxide impregnation toward controlled release of timolol maleate. J. Supercrit. Fluids 131, 11–18. https://doi.org/10.1016/j.supflu.2017.08.010.